Supporting Information

High-Output, Thermally Resilient Nano-TiO_2 Dielectric Gel Triboelectric Nanogenerator for Energy Harvesting and Reliable Temperature-Independent Pressure Sensing

Hyosik Park[a,†], Yeonkyeong Ryu[a,†], Hyeonseo Joo[a], Sujeong Gwak[a], Gbadam Gerald Selasie[a], Simiao Niu[b], Ju-Hyuck Lee*[,a,c]

[a] Department of Energy Science and Engineering, DGIST, 333, Techno Jungang-daero, Hyeonpung-eup, Dalseong-gun, Daegu, 42988, Republic of Korea

[b] Department of Biomedical Engineering, Rutgers University, Piscataway, NJ 08854, USA

[c] Energy Science and Engineering Research Center, Daegu Gyeongbuk Institute of Science and Technology (DGIST), 333 Techno Jungang-daero, Hyeonpung-eup, Dalseong-gun, Daegu 42988, Republic of Korea

[†]The authors contributed equally to this work.

Corresponding Author

E-mail: jhlee85@dgist.ac.kr (J.-H. Lee*)

Note S1. Electrical properties and TENG performance of Rutile TiO_2-based dielectric gel

We compared the electrical properties and TENG performance of a mixed TiO_2 gel and a rutile TiO_2 gel (**Fig. S8**). The rutile gel exhibited a slightly higher dielectric constant of 6.76 at 100 kHz, compared to 6.52 for the mixed TiO_2 dielectric gel. Additionally, the resistivity of the rutile gel was 2.3 MΩ·m, which is lower than the 2.9 MΩ·m of the mixed TiO_2 gel, indicating improved conductivity. However, the output of the rutile gel TENG was 109 V and 10 μA, which is approximately 10% lower than that of the mixed TiO_2 gel TENG. This reduction in output is attributed to the higher electrical properties of rutile, which can lead to increased leakage currents and consequently decrease the TENG output.

Note S2. Influence of coupling agent on the electrical properties and TENG output of TiO_2 dielectric gel

To evaluate the influence of improved TiO_2/PVC compatibility on the material's electrical properties and TENG performance, we incorporated a coupling agent (vinyltrimethoxysilane) into the 2 wt% TiO_2 dielectric gel at concentrations of 0, 1, 3, and 5 wt% relative to the mass of TiO_2 (**Fig. S10**). SEM and FT-IR analyses revealed that the coupling agent improved the dispersion of TiO_2 nanoparticles, resulting in a more uniform internal morphology. This improved dispersion, along with the polar property of the coupling agent, enhanced the dielectric constant and electrical conductivity by increasing the number of conductive paths within the material. However, this improvement was accompanied by an increase in leakage current, which increased proportionally with coupling agent concentration, peaking at 6 μA at 5 wt%. Simultaneously, the TENG output decreased as the coupling agent concentration increased, with the output dropping from 121 V and 11.1 μA at 0 wt% to 68 V and 6.3 μA at 5 wt%. These results underscore the trade-off between enhanced compatibility and reduced TENG performance, highlighting the need for optimization to achieve a balance between these factors.

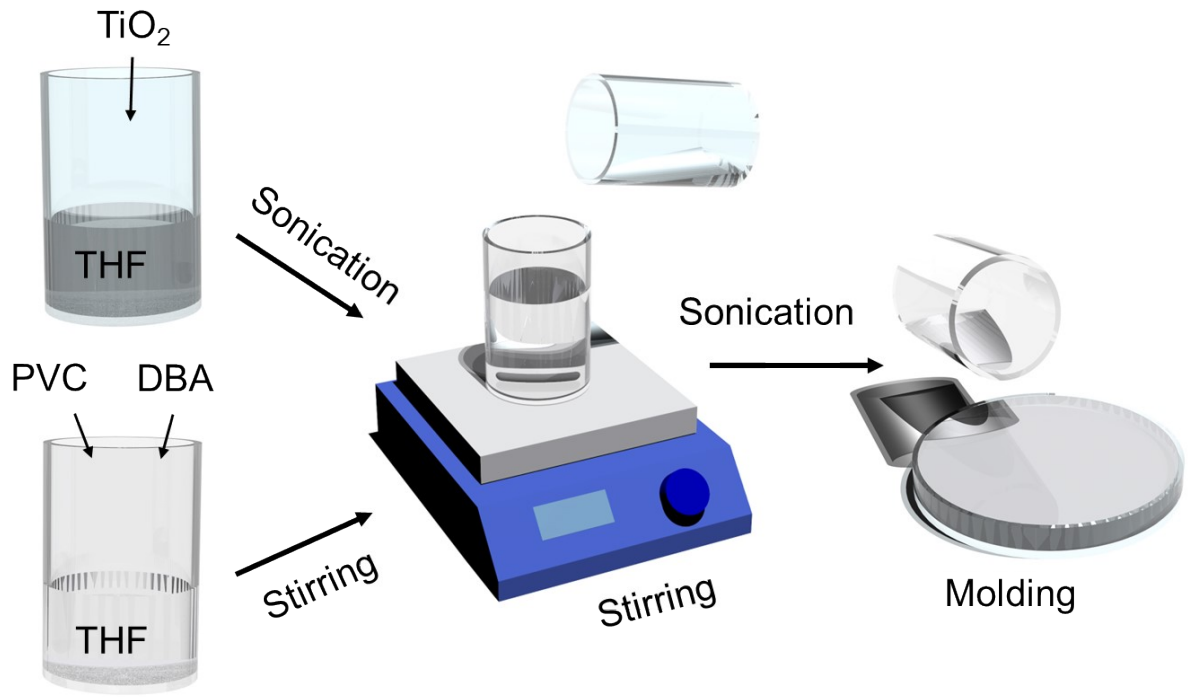

Fig. S1. Fabrication process of TiO_2 PVC gels.

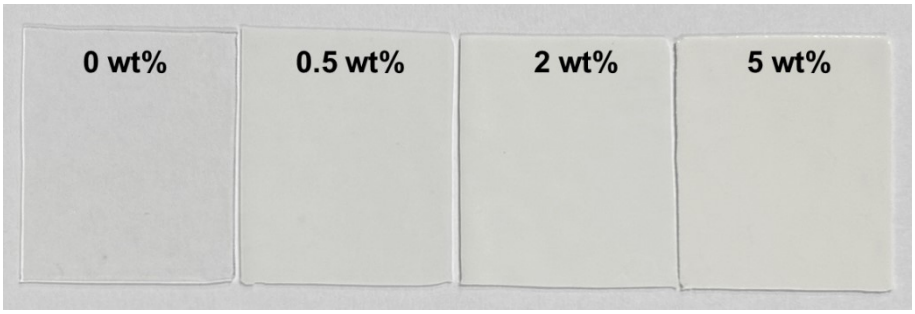

Fig. S2. Photographs of PVC gel and TiO_2 PVC gels.

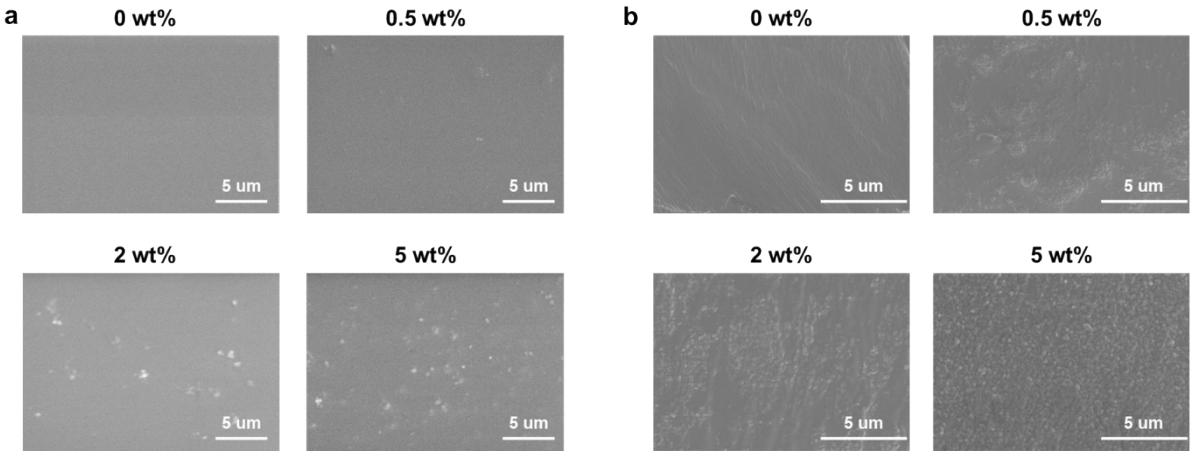

Fig. S3. (a) Surface SEM images of PVC gel and TiO_2 PVC gels. (b) Cross sectional SEM images of PVC gel and TiO_2 PVC gels.

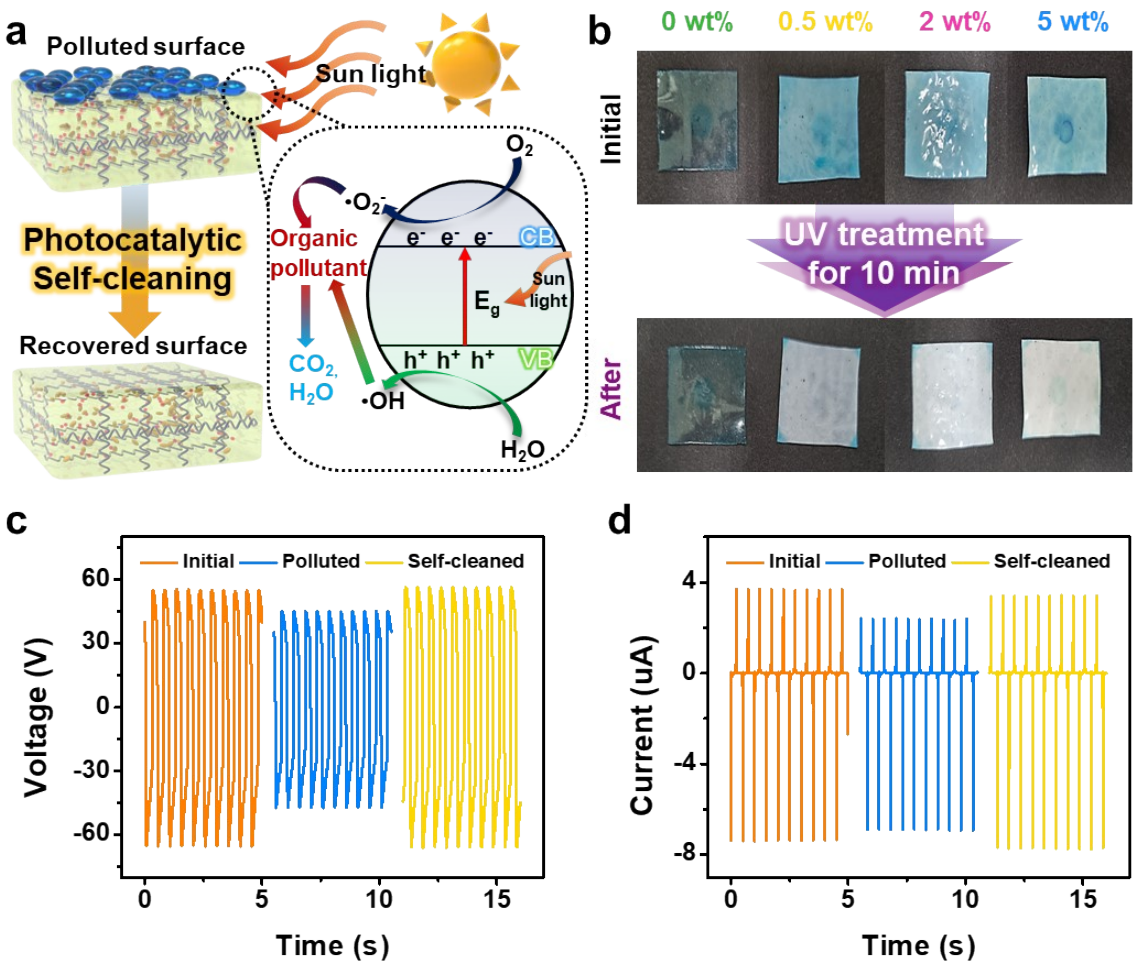

Fig. S4. Self-cleaning ability of TiO_2 dielectric gels. (a) Self-cleaning mechanism of TiO_2 photocatalytic properties. (b) Photographs of the self-cleaning effect of UV irradiation on PVC gel and TiO_2 dielectric gel contaminated with methylene blue. c-d. (c) output voltage and (d) output current of 2 wt% TiO_2 dielectric gel contaminated with methylene blue before and after UV irradiation-induced self-cleaning.

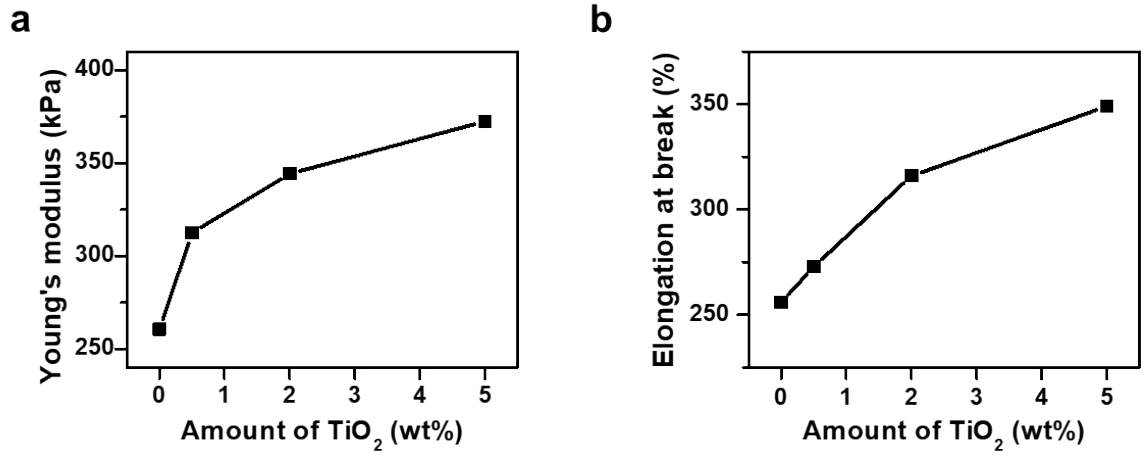

Fig. S5. Mechanical properties of PVC gel and TiO_2 PVC gels. (a) Young's modulus of TiO_2 PVC gels at 0 wt%, 0.5 wt%, 2 wt%, and 5 wt%. (b) Elongation at break of TiO_2 PVC gels at 0 wt%, 0.5 wt%, 2 wt%, and 5 wt%.

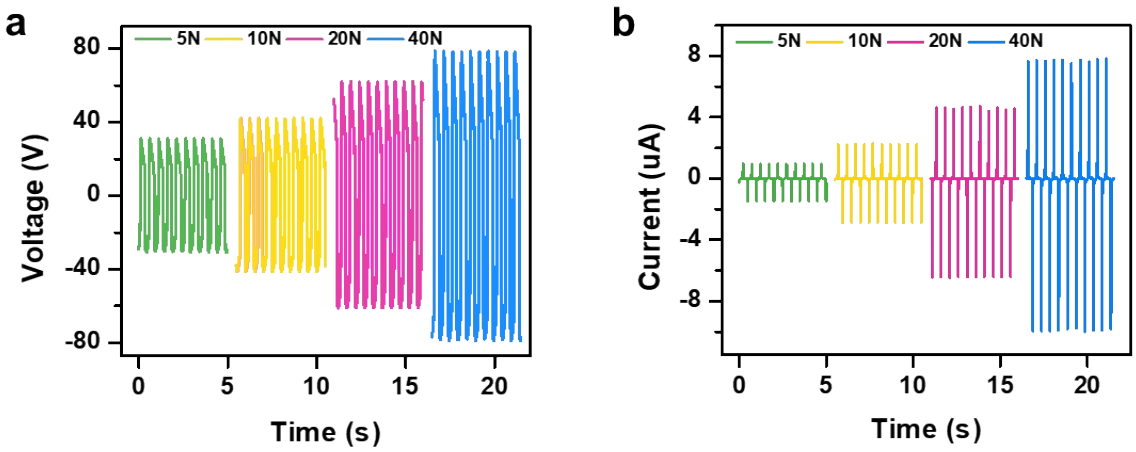

Fig. S6. Output performance of 2 wt% TiO_2 TENG under varying pressure. (a) Output voltage and (b) current over pressures from 5 N to 40 N.

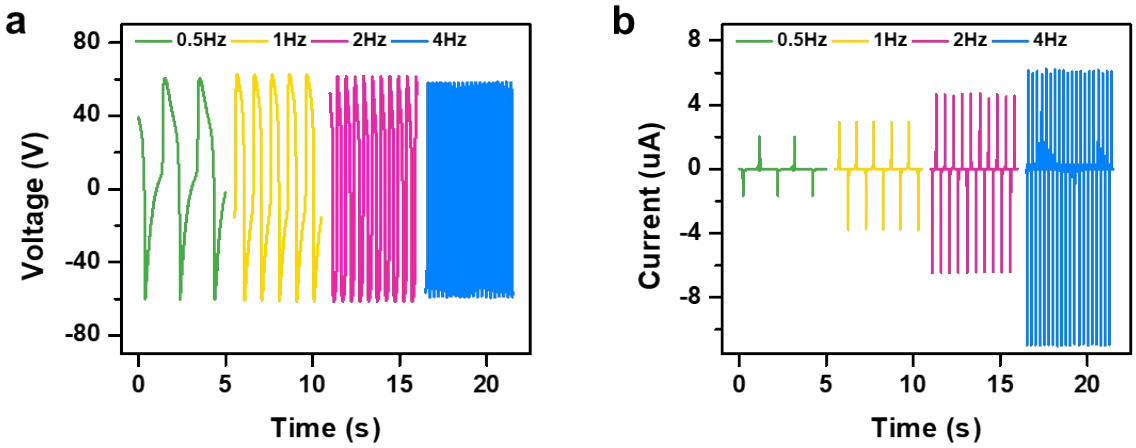

Fig. S7. Output performance of 2 wt% TiO_2 TENG at varying frequency. (a) Output voltage and (b) current across frequencies from 0.5 Hz to 4 Hz.

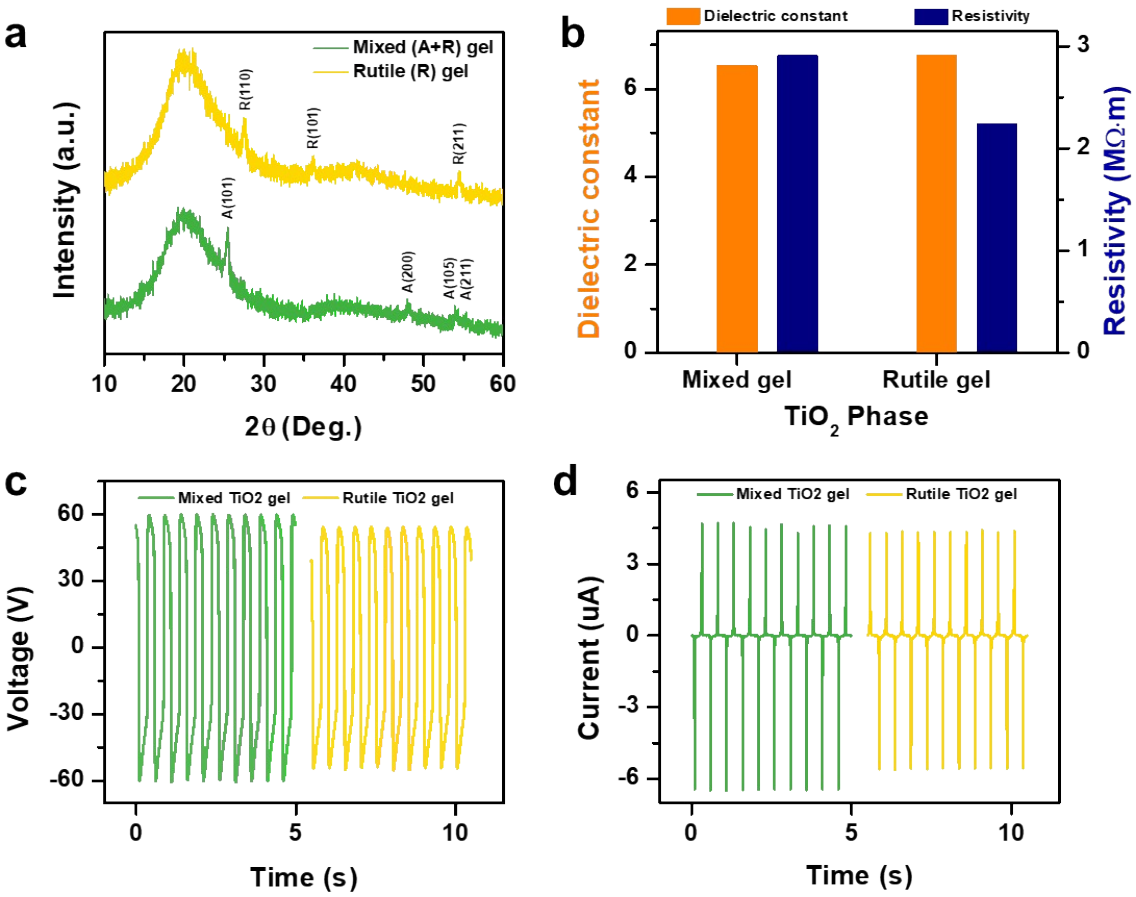

Fig. S8. Comparison characteristics and TENG output performance between 2 wt% mixed-phase and 2 wt% rutile-phase TiO_2 dielectric gels. (a) XRD patterns of mixed-phase and rutile-phase gels. (b) Dielectric constant and resistivity of mixed and rutile gels. c-d. TENG output performance of mixed and rutile gels: (c) output voltage and (d) output current.

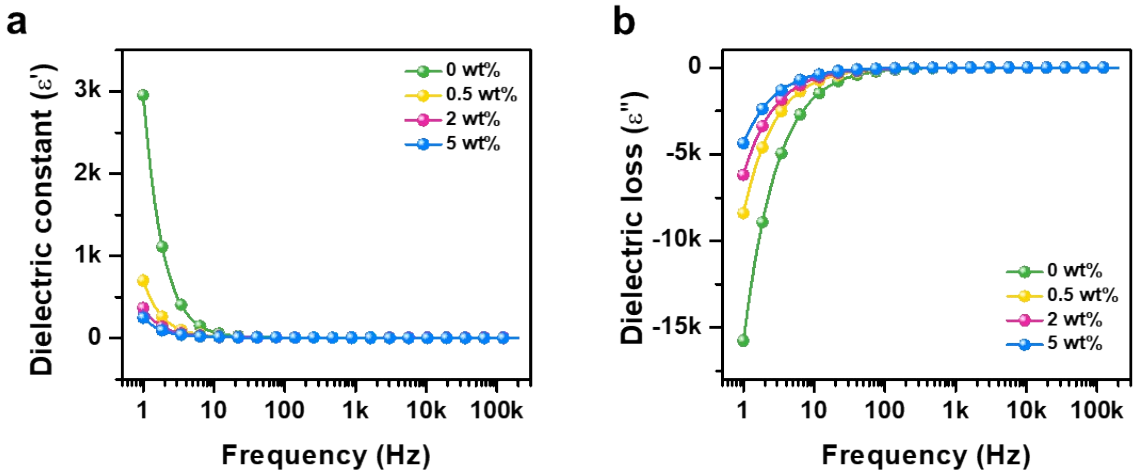

Fig. S9. Dielectric properties of PVC gel and TiO_2 PVC gels. (a) Dielectric costant and (b) dielectric loss by frequency from 1 Hz to 200 kHz.

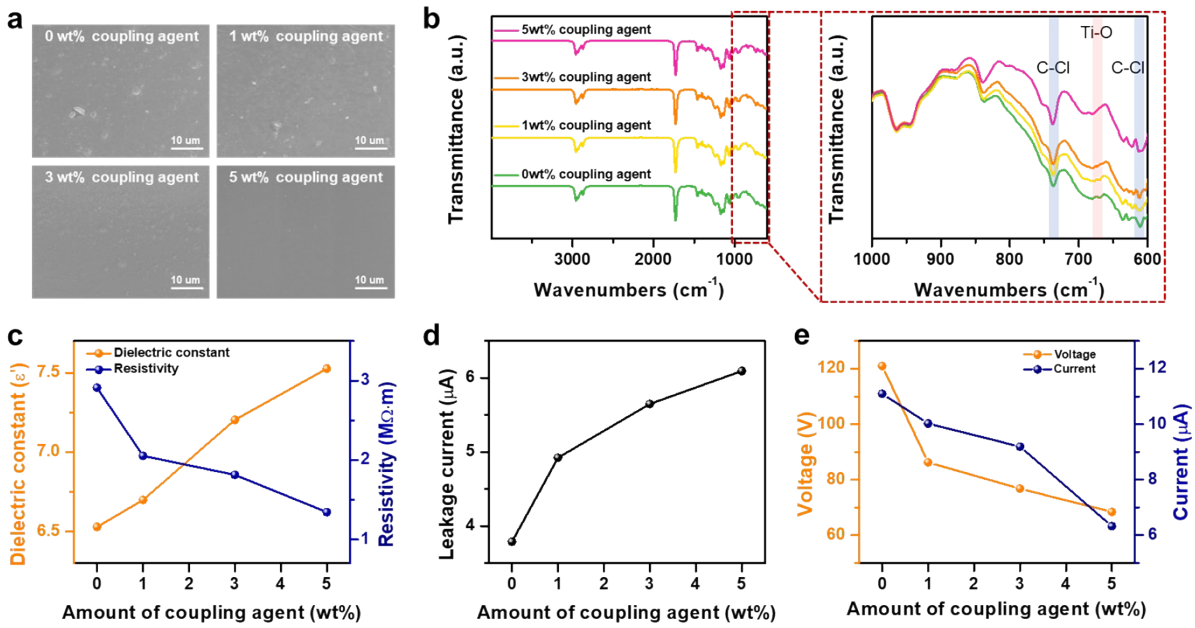

Fig. S10. Electrical properties and TENG output performance of 2wt% TiO_2 dielectric gel with different coupling agent concentrations. a-b. (a) SEM images and (b) FT-IR spectra of the TiO_2 dielectric gel with 0 to 5 wt% coupling agent ratios. (c) Dielectric constant and resistivity of the TiO_2 dielectric gel with different coupling agent ratios. d-e. (d) Leakage current and (e) output performance of the TiO_2 dielectric gel with 0 to 5 wt% coupling agent ratios.

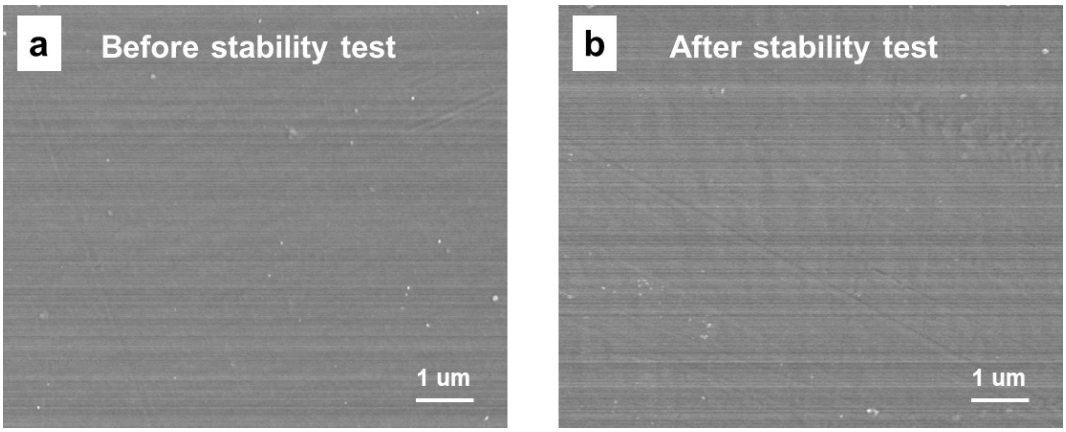

Fig. S11. Evaluation of plasticizer transfer after 5,000 cycles stability test. a-b. Nylon surface SEM images of (a) before and (b) after stability test.

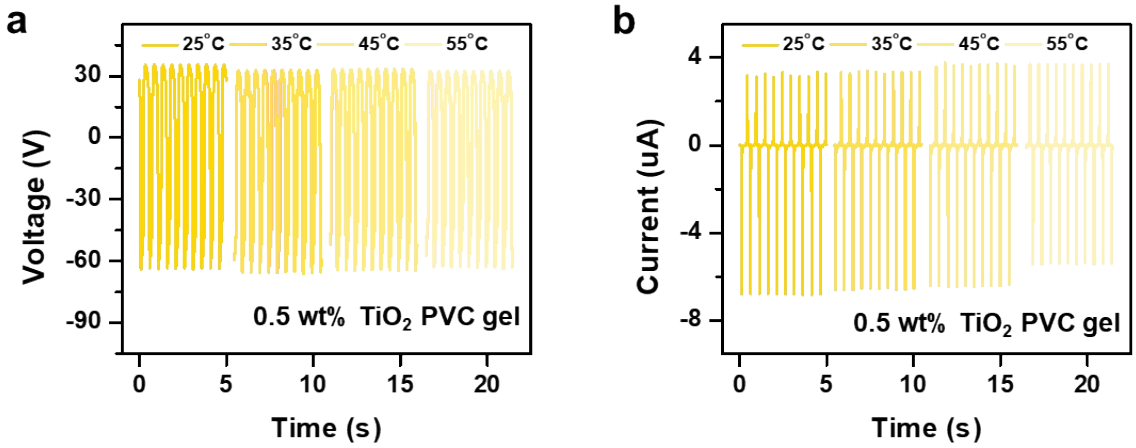

Fig. S12. Output performance of 0.5 wt% TiO_2 PVC gel TENG at varying temperatures. (a) Output voltage and (b) current across temperatures from 25°C to 55°C.

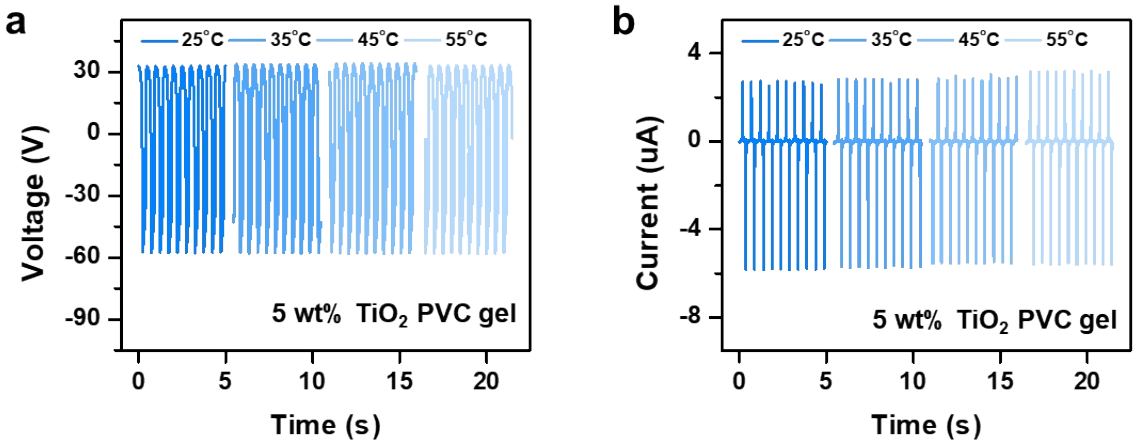

Fig. S13. Output performance of 5 wt% TiO_2 PVC gel TENG at varying temperatures. (a) Output voltage and (b) current across temperatures from 25°C to 55°C.

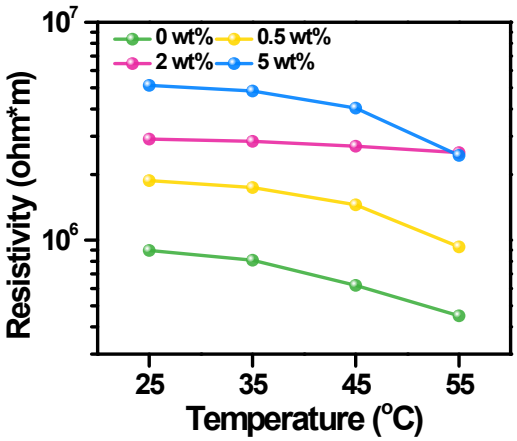

Fig. S14. Resistivity of PVC gel and TiO_2 PVC gels by different temperatures (25°C-55°C)

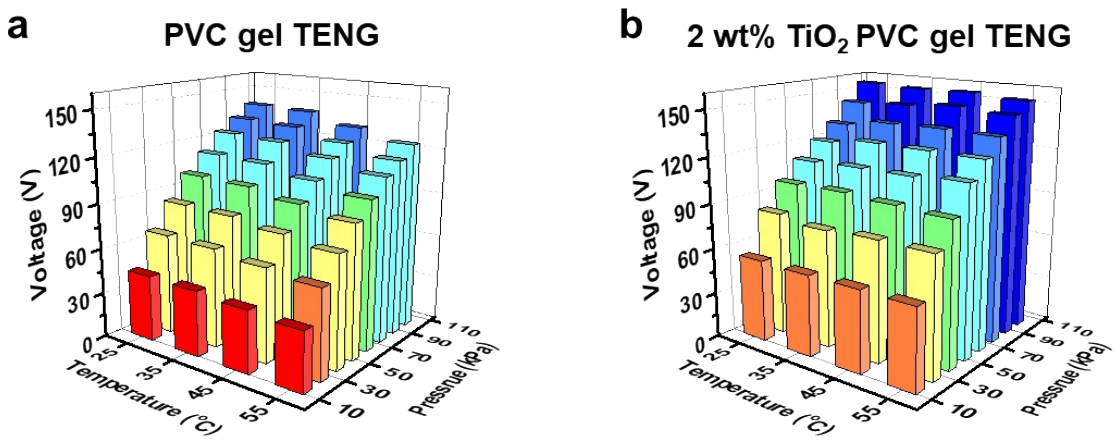

Fig. S15. Output performance of TENGs by different temperature and pressure. (a) PVC gel TENG output voltage and (b) 2 wt% TiO_2 PVC gel TENG output voltage.

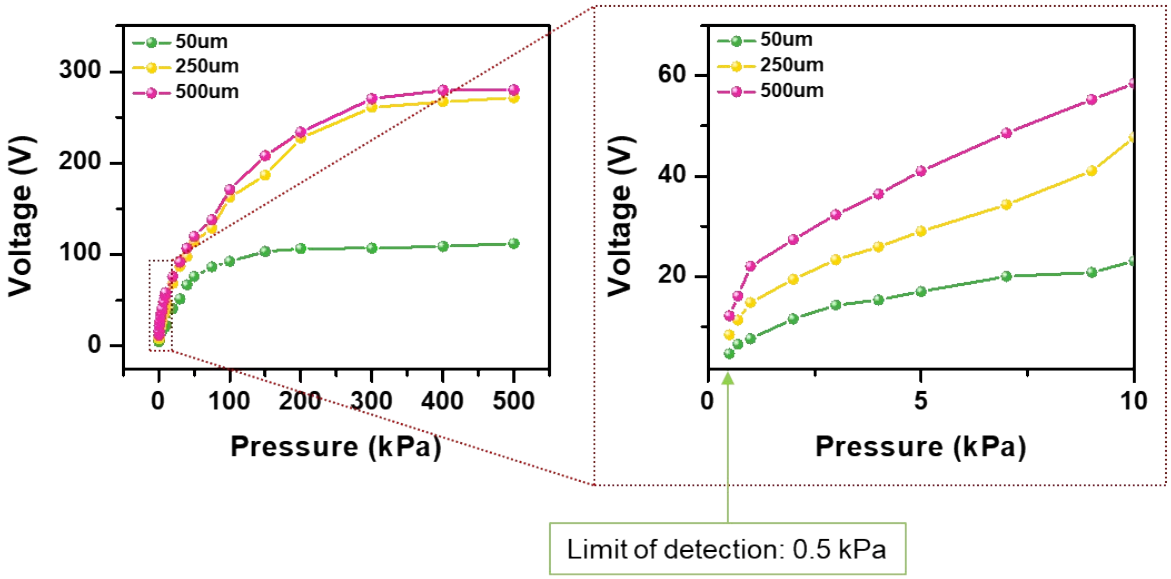

Fig. S16. Output voltage from 2 wt% TiO_2 PVC gels with thicknesses of 50 µm, 250 µm, and 500 µm across a pressure range from 0.5 kPa to 500 kPa.

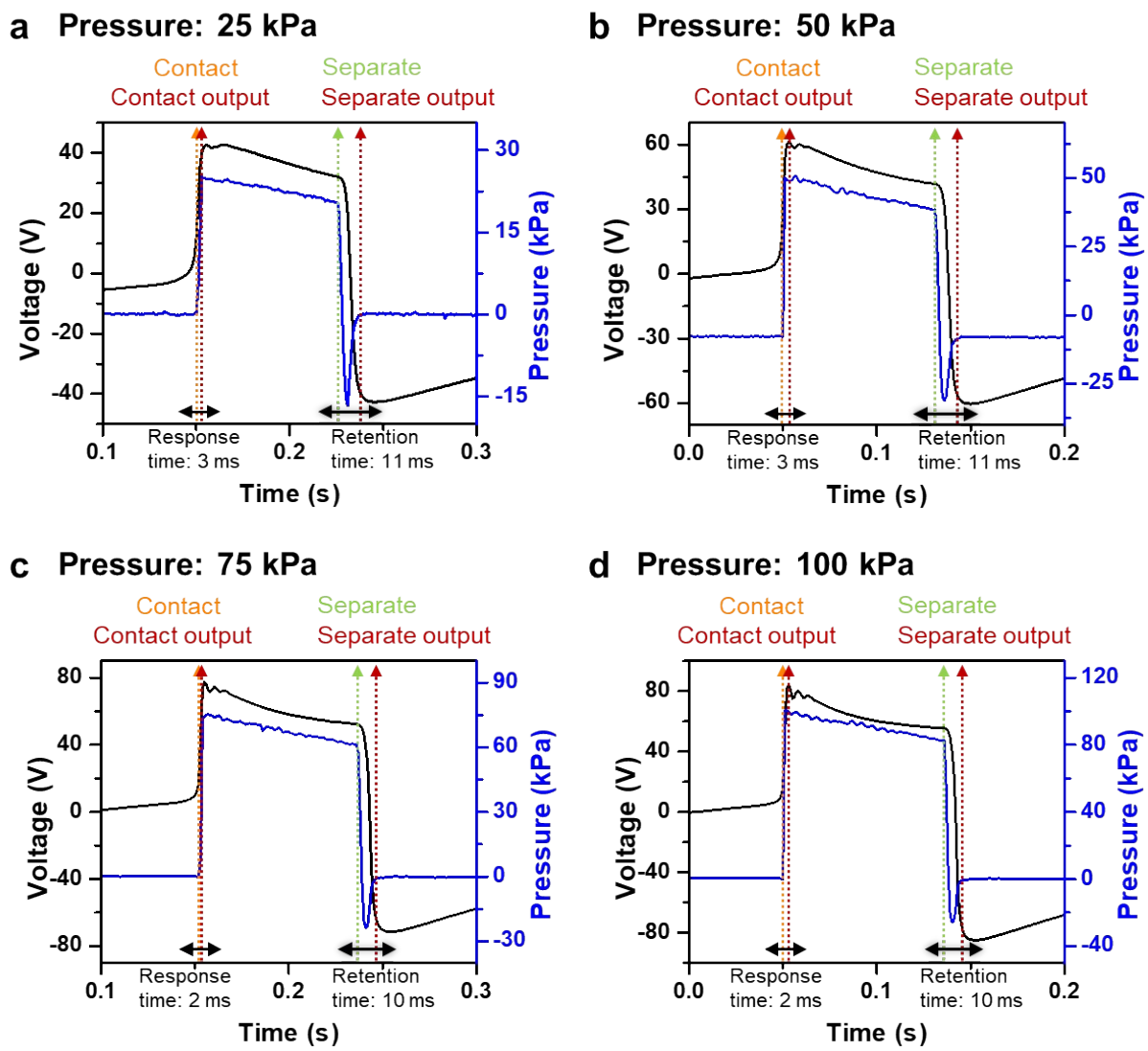

Fig. S17. Response time and retention time of sensing applications based on 2 wt% TiO_2 PVC gel TENG at varying pressure. (a) applied pressure 25 kPa, (b) 50 kPa, (c) 75 kPa, (d) 100 kPa.

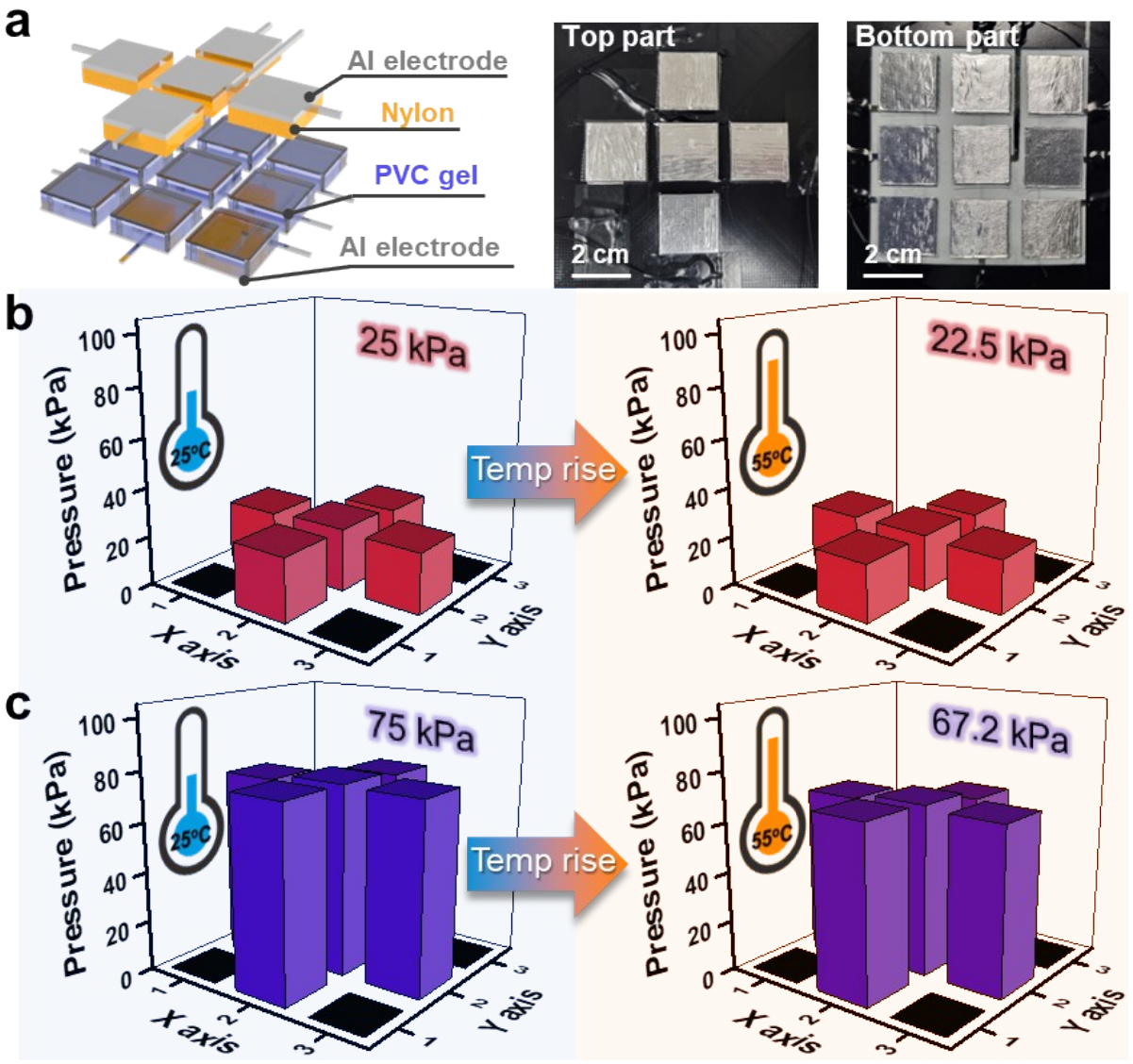

Fig. S18. Pressure sensing application based on PVC gel TENG with plus sign shaped top part. (a) Schematic and photographs of the pressure sensor. (b) Sensing accuracy of the sensor under applied pressure 25 kPa and (c) 75 kPa at 25°C and 55°C.

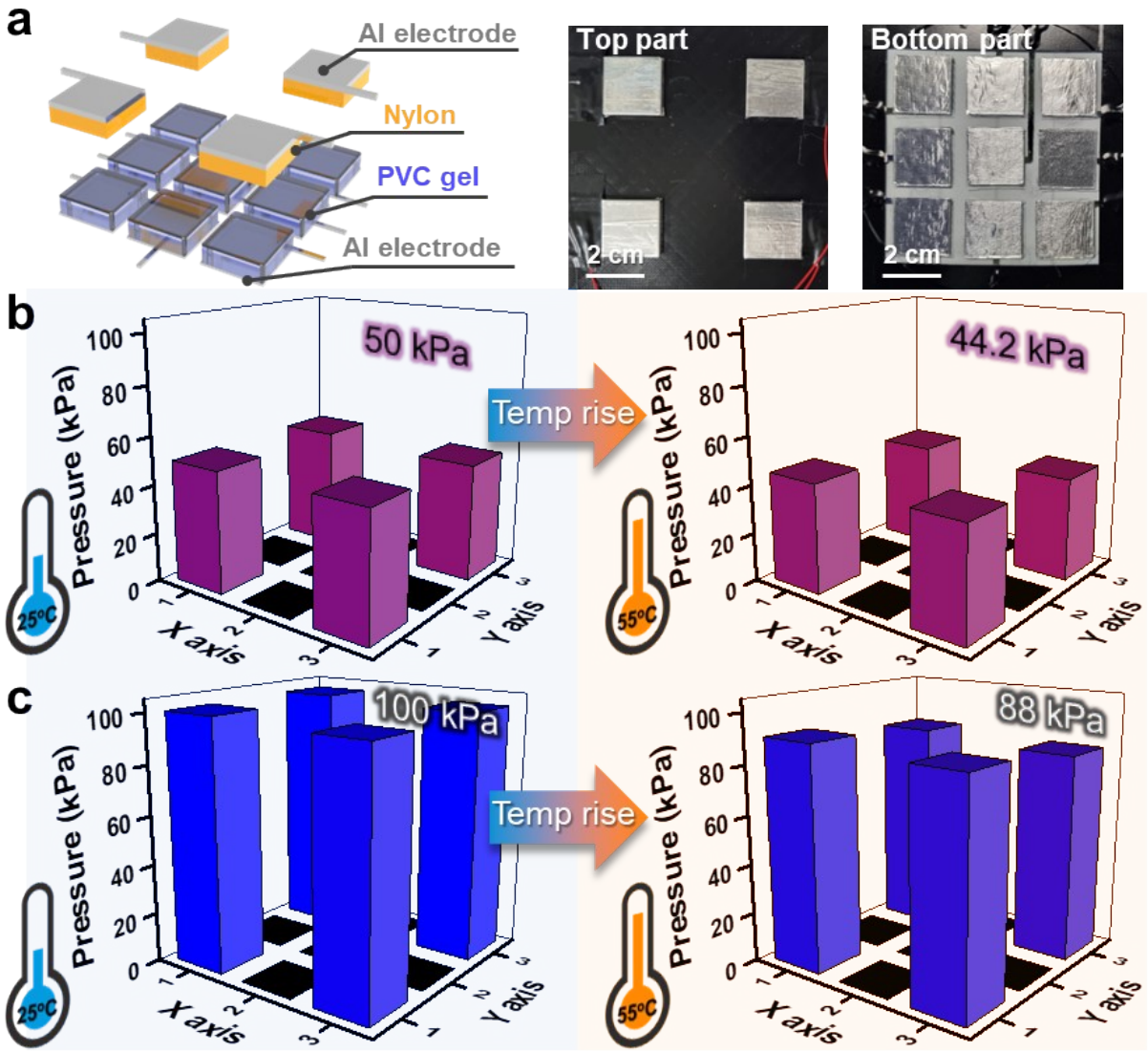

Fig. S19. Pressure sensing application based on PVC gel TENG with square shaped top part. (a) Schematic and photographs of the pressure sensor. (b) Sensing accuracy of the sensor under applied pressure 50 kPa and (c) 100 kPa at 25°C and 55°C.

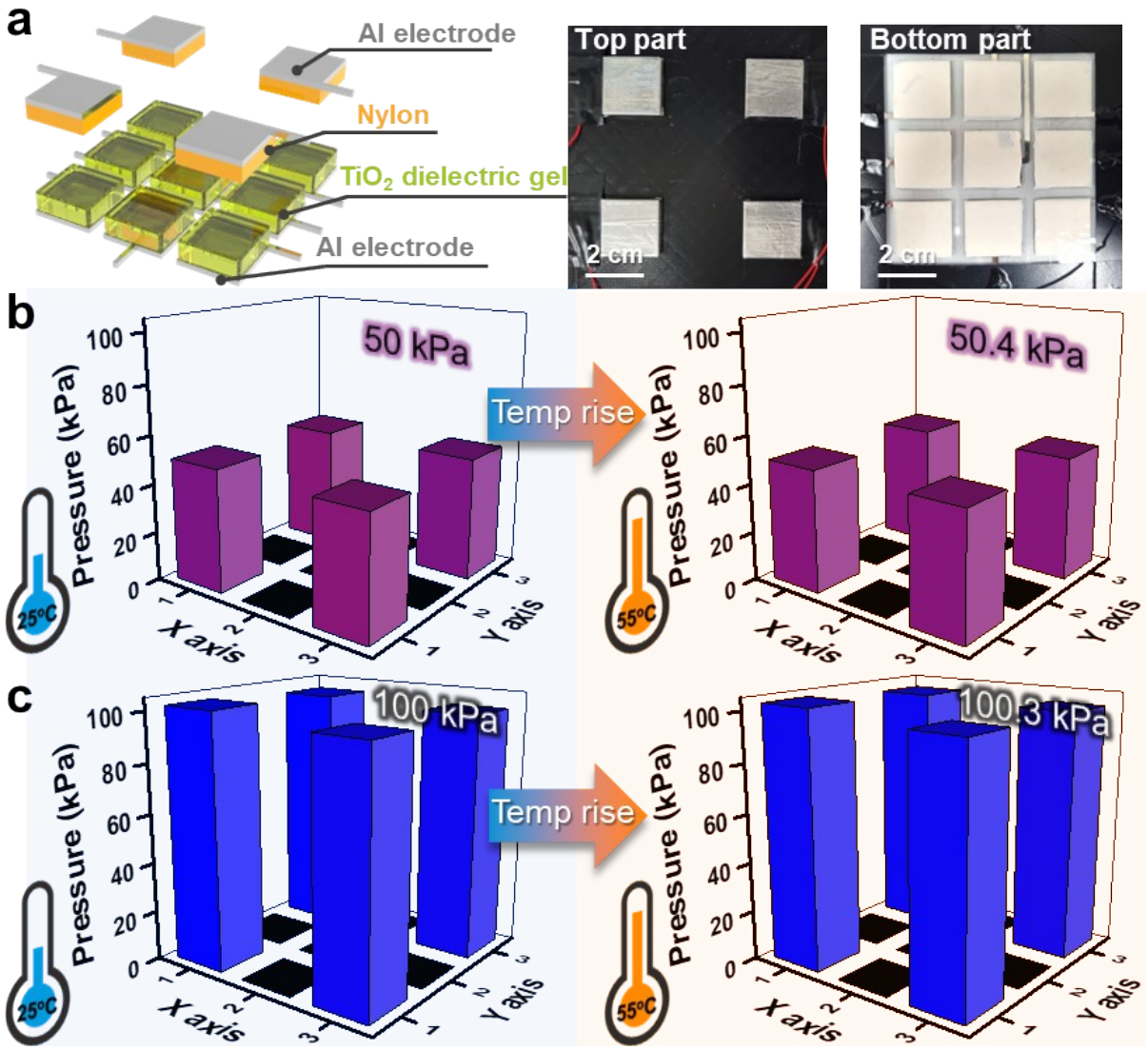

Fig. S20. Pressure sensing application based on 2 wt% TiO_2 PVC gel TENG with square shaped top part. (a) Schematic and photographs of the pressure sensor. (b) Sensing accuracy of the sensor under applied pressure 50 kPa and (c) 100 kPa at 25°C and 55°C.

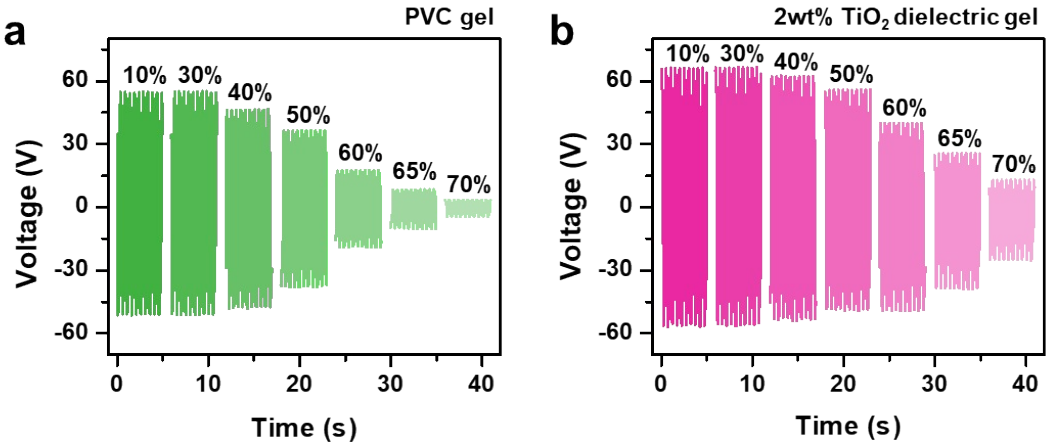

Fig. S21. Output performance of TENGs in different humidity environments. Output voltage variations of (a) PVC gel TENG and (b) 2 wt% TiO_2 dielectric gel across a humidity range of 10% to 70%.

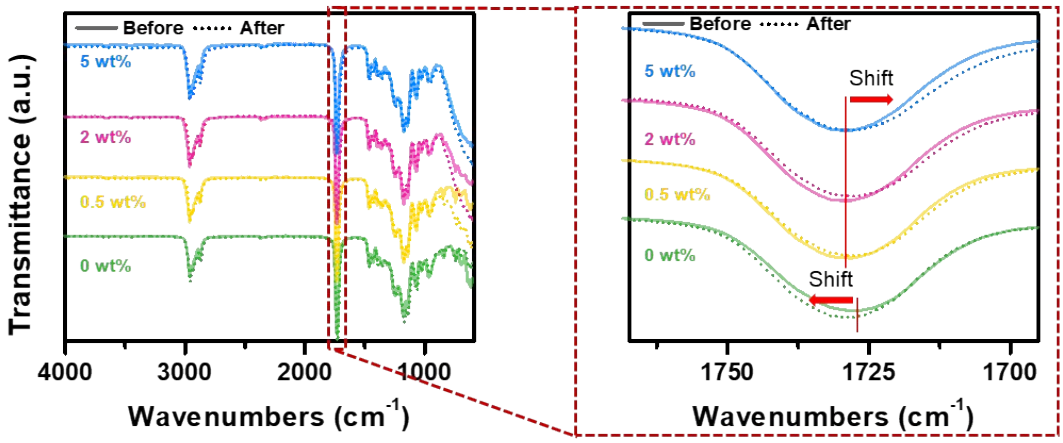

Fig. S22. FT-IR peak of PVC and TiO_2 PVC gels before (straight line) and after (dot line) 7 days thermal test at 60°C.

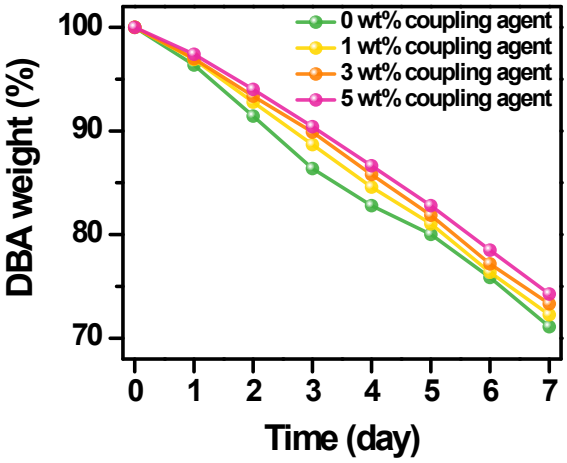

Fig. S23. DBA weight change of TiO_2 dielectric gels with different ratios of coupling agents (0, 1, 3, 5 wt%) over time at 60 °C.